Interaction Models for Nb/AlOx/Nb Josephson Junctions

Alin Airinei, Zachary Kluger*
Department of Physics, Stony Brook University, Stony Brook, NY 11794
(Dated: April 2020)

To analyze the superconducting properties of the pure metal Niobium we used liquid helium to cool down a probe Nb/AlOx/Nb Josephson Junction to temperatures much smaller than the transition-temperature T_c, and determined our experimental results by analyzing the junction I-V characteristics. Our goal is to measure the temperature dependence of the energy gap and supercurrent, and compare our results with established electron pair interaction models, and with data from similar experiments.

I. Introduction

I.1. Theory

BCS - the standard model

The Bardeen-Cooper-Schrieffer(BCS) formalism is one of the earliest and most tested microscopic frameworks of superconductivity. It's main prediction is the formation of *Cooper pairs* at low temperatures which propagate through the lattice with zero resistance due to electron-phonon interaction [1].

The number of conduction electrons in a regular conductor tends to zero as the temperature goes to $T = 0$. In contrast, as the temperature of a superconductor decreases, more free electrons are forming pairs with opposite spins and net spin zero (compound bosons) which will simultaneously create a energy gap 2Δ in the energy spectrum of the free electrons, analogous to the band gap in a semiconductor [1, 3].

As a consequence of the energy gap, the electrons that are not in the ground (superconductive) state can no longer move with zero resistance. This explains why superconductors are in general poor conductors at high temperatures, as the gap energy is the energy required to break a Cooper pair apart [1].

The BCS theory is particularly accurate for *weak-coupling interactions* near the transition temperature T_c (small energy gap). At $T = 0$ the theory predicts [1, 2, 3]:

$$\Delta(0) \approx 1.764 k_B T_c \tag{1}$$

which yields a numerical value of $\Delta(0) = 1.406 meV$ for a total gap energy of $2\Delta = 2.81 meV$. This values can be checked by spectroscopy as photons with the right energy will be absorbed [1].

For higher temperatures near T_c(weak-coupling), the theory predicts[1, 3]:

$$\delta = 1.74(1 - t^2)^{1/2} \tag{2}$$

where: $\delta \equiv \Delta(T)/\Delta(0)$, and $t = T/T_c$ is the reduced temperature [3, 4]. This result does not hold for strong-coupling interactions and a much accurate approximation as given by [2, 4] is:

$$\delta^2 \equiv \left[\frac{\Delta(T)}{\Delta(0)}\right]^2 = cos(\frac{\pi t^2}{2}) \equiv sin(\frac{\pi}{2}(1 - t^2)) \tag{3}$$

In this experiment we analyze I-V characteristics and temperature-dependent properties of Nb/Nb tunnel junctions (Josephson junctions) for gap regions ranging from strong to weak coupling interactions (from $T \approx 4.2K$ to near $T = T_c = 9.25K$).

Josephson Junctions

Josephson Junctions are most basically fabricated as trilayers of a superconducting material, a barrier, and another superconducting layer. The barrier can be a thin insulator (SIS) or a normal-metal (SNS), as well as other states in-between [10].

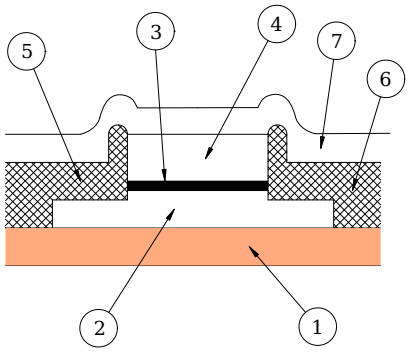

1	Si Substrate
2	Nb Base Electrode
3	Al_2O_3 Tunnel Barrier
4	Nb Counter Electrode
5	SiO_2 Insulation
6	SiO_2 Insulation
7	Nb Wiring

Figure 1. Schematic view of the cross-section of a $NbAl_2O_3Nb$ tunneling junction. Design concepts were borrowed from [5, 6, 7, 8, 9].

* alin.airinei@stonybrook.edu
zachary.kluger@stonybrook.edu

The junctions used for our experiment have been fabricated by self-aligned lift-off of a PMMA bilayer resist, and UVN-30, using UV and electron beam lithography(EBL), as well as reactive-ion etching(RIE) in SF_6 plasma. The layers are sputtered on a Si substrate with the base Nb electrode at 150nm thickness, the Al_2O_3 barrier at 8-10nm, and the third layer (counter electrode) at 150nm thickness[6].

As shown in Figure 1.(not to scale), after the final etching of the base and counter electrodes, a 160-170nm layer of insulating SiO_2 is deposited to seal the layers and prevent any shorts. The top of the insulating layer is then removed to expose the counter electrode and a final 250nm wiring layer is added to complete the design [6, 7].

I.2. Setup and Methodology

Experimental Setup

Our apparatus consisted of the cryostat probe, the pumping system, differential amplifiers, reference resistors, a DC voltage source, a decade resistor, a Wavetek sweep generator, an HP digital oscilloscope, two multimeters, and power supplies for the heater and the magnet.

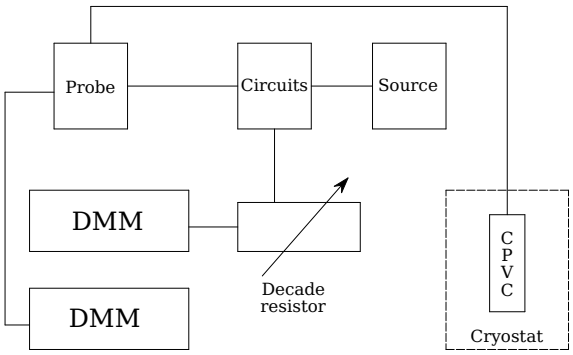

Figure 2. The diagram shows the temperature measuring part of the experimental setup. The *Cryogenic Probe Vacuum Can* (CPVC) contains enclosed the test circuitry including the germanium thermometer and the Josephson junctions.

The decade resistor was used to measure the temperature within the probe, which was submerged in liquid He. To take the I-V measurements we used the sweep generator and the multimeters. The sweep generator was connected to the reference resistors which were then connected to the cryostat probe. The probe then connected to the differential amplifiers, then the multimeters, and finally the oscilloscope. The multimeters were connected at the same time to the LabView VI interface.

Methods

To take all of our measurements we used LabView VI attached to the rest of the apparatus. To determine the resistance within the junction we measured the voltage through the circuit and used a decade resistor to alter the resistance in an identical circuit. Using this reading we were able to use the resistance-temperature curve of the germanium thermometer in the superconductor probe to determine the temperature of the probe. To alter the temperature in the junction, we increased the current. We then recorded the I-V curve of the junction at each current and used this data to determine the temperature dependence of the gap voltage and the Josephson current.

II. Results

Temperature Measurements

To determine the temperature of the probe we compared the measured resistance values with the known response curve of the germanium sensor [3]. The graph below shows the temperature correspondence with the resistance values and our measured temperature range with values between 10.5K to 4.354K.

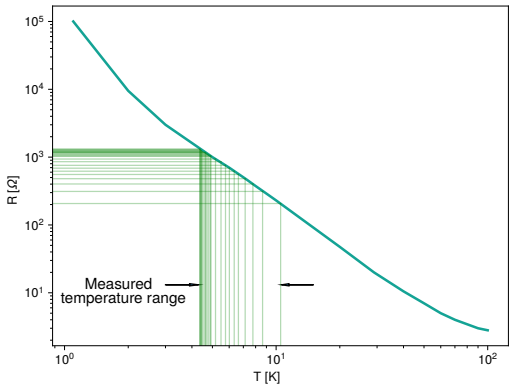

Figure 3. The graph is a reproduction of the original response curve for the Lake Shore Cryotronics germanium temperature sensor (GR-200A-1500) as published in[3].The reproduction was made to facilitate the determination of the temperature values corresponding to the measured resistance values by graphical analysis.

Tunneling Characteristics

Fig. 4 shows the current-voltage characteristics of our test junction at T=4.35K, with the temperature measured by the procedure explained in the previous section. The expected features of tunneling junctions with identical electrodes are observed. At sub-gap voltages there is a "zero-voltage" or Josephson current flow, while in the

quasiparticle region above the gap energy we observe an increase in tunneling current.

In the case pictured above, we measured a maximum Josephson current of $12.78 \pm 0.31 \mu A$ which, with a normal-state resistance measured from $\Delta I/\Delta V$ at $V > 2\Delta/e$ of 124.08 ± 0.29, gives a characteristic voltage $I_c R_n$ value of $\approx 1.60 \pm 0.04 mV$. In the next two sections we will discuss the results of analyzing the IVC data for all measured temperatures focusing on the variation of gap voltage and Josephson current with temperature while comparing our results with the weak and strong interaction models.

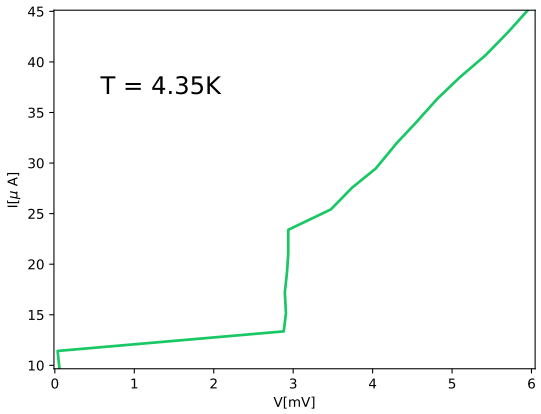

Figure 4.

Temperature Dependent Properties

Gap Voltage

The gap voltage within the junction corresponds to the energy that is required to break apart Cooper pairs. As the temperature gets closer to T_c, the gap voltage decreases. This decrease in gap voltage shows us that the bond between the two electrons in the Cooper pair gets weaker as we approach T_c. This also indicates that the charge carriers are in fact the Cooper pairs because it shows a collective nature in the charge carriers that disappears above the critical temperature.

When the Cooper pairs are broken, the energy supplied to each electron must be at least equal to that of the energy gap. As such, an energy of twice this is supplied to the superconductor. This value, $2\Delta/e$, is the voltage corresponding to the current jump on the I-V curve (i.e. the transition between the Josephson to the quasiparticle branches of the curve).

This data (Fig. 5) agrees fairly well with the BCS strong coupling model at low temperatures, whereas the weak coupling model blows up. At higher temperatures closer to T_c, the weak coupling model begins to agree with the strong coupling approximation.

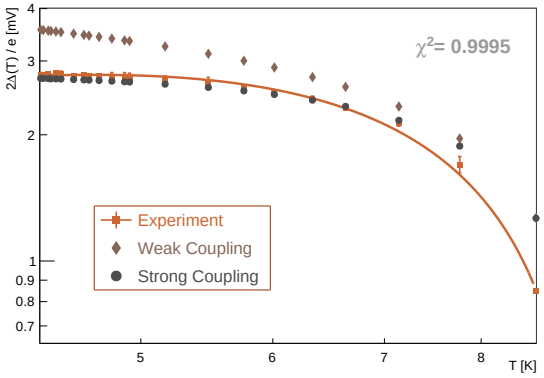

Figure 5. The variation of gap voltage with temperature. The weak coupling (Eq.(2)), and strong coupling (Eq. (3)) interaction models, with $\Delta(0)$ from Eq. (1), compared with the experimental data (solid line).

Josephson Current

Having proven the generality and fair agreement of Eq. (3) with the experiment we employed its results to test another formulation which establishes the relation between the Josephson current, the gap voltage, and the normal state resistance R_n.

The formula, commonly known as the Ambegaokar-Baratoff result, as given in [3, 11], is:

$$I_c = \frac{\pi}{2} \frac{\Delta(T)}{eR_n} tanh(\frac{\Delta(T)}{2k_B T}) \tag{4}$$

We employed (4) in a quasi-empirical manner, as the R_n value, not known in advance, or measured otherwise, was determined from the IVC by averaging samples in both directions of the sweep at voltages above the gap voltage.

We determined the conductance in this manner for each temperature and thus determined that the variation of R_n with temperature is insignificant, except in the close vicinity of T_c.

We used this result together with $\Delta(T)$ obtained from Eq. (3) to calculate the temperature dependence of I_c using Eq. (4) and compared the results with the experimental values as shown in Fig. 6.

We notice from the results that the "weak" model is far off, as expected, and was only included in our analysis for completeness. The "strong" model also gives higher current values than actually observed.

Such discrepancies are usually observed in similar experiments, in resistive and non-resistive settings, such as discussed in [10, 11]. This seems to indicate that Eq. (4), as it is, only offers a rough approximation of the current variation with temperature.

Among other factors that can contribute to the disagreement, beside the cumulative approximation errors of Eqs. (4) and (3), are possible errors on our end which may include an underestimation of R_n, an

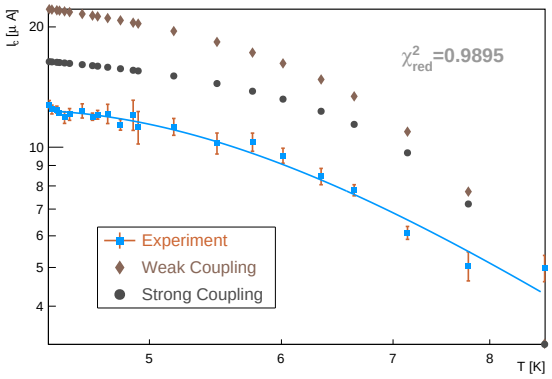

Figure 6. The Josephson current vs temperature. The solid line shows the experimental results. The weak and strong points are calculated from Eqs. (2), (3), and (4.)

underestimation of T, critical field effects, thermal noise, junction material and size, design specific characteristics, as well as instrument calibration and precision.

The self induced critical fields are of particular interest [1, 11], while the junction specific characteristics (such as barrier thickness, material, and fabrication defects, etc.) might yield better results for some junctions rather than others [10]. A general trend in most cases is that (4) seems to always yield higher estimations compared to the experimental values.

III. Conclusions

We first analyzed the dependence of the gap voltage on temperature. This data showed that the strong coupling model fits better with the Nb/AlOx/Nb Junction than the weak coupling model at low temperatures. At higher temperatures closer to T_c, both models agree with the experimental data, showing that near T_c the BCS theory is a good approximation.

We then examined the dependence of the Josephson current, I_c, across a range of temperatures. As expected we found that there was more current as temperature decreased. Using this data we again tested the strong and weak coupling models against the Ambegaokar-Baratoff formula and showed that, once again, the results do not perfectly align with the theory.

We conclude that a purely analytical approach does not account for all observed behavior, and corrections are called for (either theoretical or experimental) to characterize a particular junction design or fabrication process.

Acknowledgments

The authors would like to thank Dr. Mengkun Liu and Gleb Aminov for assisting in the setup and theory of the experiment, as well as Justin Ao and Jeremy Schleiffer for aiding in the collection of data.

[1] Stephen T. Thornton and Andrew Rex, Modern Physics for Scientists and Engineers, 4th ed. (CENGAGE LEARNING, Boston, MA, 2013).

[2] T. P. Sheahen, Physical Review 149, 370 (1966).

[3] Department of Physics and Astronomy at Stony Brook University. *Superconductivity in Niobium.* Experiment Write-up, Revised Oct. 09, 2006.(Unpublished).

[4] T. P. Sheahen, Physical Review 149, 368 (1966).

[5] Michael Gurvitch. *Short Introduction to Tunneling.*2002. (Unpublished).

[6] V. Patel, W. Chen, S. Pottorf, and J. Lukens, IEEE Transactions on Appiled Superconductivity 15, 117 (2005).

[7] M. B. Ketchen, D. Pearson, A. W. Kleinsasser, C. K. Hu, M. Smyth, J. Logan, K. Stawiasz, E. Baran, M. Jaso, T. Ross, K. Petrillo, M. Manny, S. Basavaiah, S. Brodsky, S. B. Kaplan, W. J. Gallagher, and M. Bhushan, Applied Physics Letters 59, 2609 (1991).

[8] M. Ohkubo, J. Martin, K. Drachsler, R. Gross, R. P. Huebener, I. Sakamoto, and N. Hayashi, Physical Review B 54, 9484 (1996).

[9] L. Fritzsch, H.-J. Khler, F. Thrum, G. Wende, and H.-G. Meyer, Physica C: Superconductivity 296, 319 (1998).

[10] V. Lacquaniti, D. Andreone, S. Maggi, R. Rocci, A. Sosso, and R. Steni, Physica C: Superconductivity and Its Applications 435, 99 (2006).

[11] R. F. Broom, Journal of Applied Physics 47, 5432 (1976).